Traction Control for a PM Axial-Flux In-Wheel Motor

Conference presentation: the present paper was presented at the conference EPE-PEMC 2007

***Abstract*—The traction control is a tool to increase stability and safety of vehicles and it has a greater performance potential in electrical vehicles than in ICV. Moreover, the traction control allows the EV to operate more efficiently preventing slippage in acceleration and permitting the use of high-efficiency low-drag tires. The presented approach can compete with the well-established techniques, but it offers a lighter tuning procedure. This paper presents an approach to the longitudinal control of a single wheel adopting a configuration based on an adherence estimator and a controller of the adherence gradient. The presented approach allows tracking of the value of the adherence derivative in a wide operating range without any knowledge of the road conditions. The work is based mainly on experimental tests. The test rig computes the vehicle dynamics in real-time and loads accordingly the drive under test. The controller was experimentally verified showing good behavior.**

I. Introduction

The traction control of road vehicles improves driving safety in difficult weather or traffic conditions as well as the stability during high performance driving. Moreover, the limitation of the slip between road and tire reduces the wear of the tires. Nevertheless, a key point is the efficiency benefit produced by the traction control, that lays mainly on the slip reduction. The efficiency influences the emission of any vehicle, but in the EV case, it is a primary concern because it influences also the range. Also, in the HEV case a better efficiency leads to an improvement of the zero emission range.

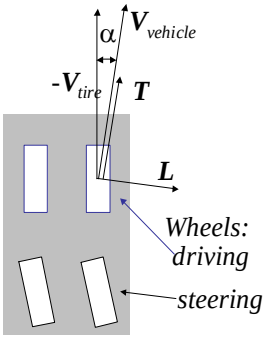

Fig. 1. Speeds and forces in tire-road contact.

In the tire-road contact, the vehicle-road speed $\boldsymbol{V}_{vheicle}$ and the tire-road speed $\boldsymbol{V}_{tire}$ differ in magnitude and direction as in Fig. 1; this contact provides two horizontal force components onto the vehicle: the driving or longitudinal force $\boldsymbol{T}$, and the side or lateral force $\boldsymbol{L}$, as shown in Fig. 1. Both components are strongly dependent on the slip, defined as:

$$\sigma = \frac{V_{tire} - V_{vehicle}}{|V_{vehicle}|}, \qquad (1)$$

and on the slip angle α, as shown by Fig. 2, where the forces are respectively expressed, as usual, through the normal force N and the driving or longitudinal friction coefficient μ and the side or lateral friction coefficient μ_L [8-10].

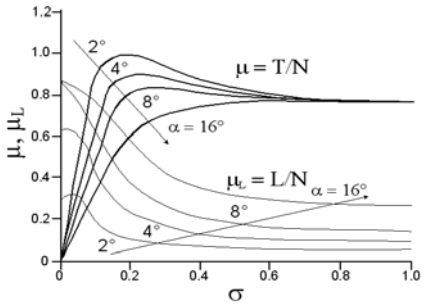

Fig. 2. Driving and side friction coefficients as function of slip and slip angle.

According to the authors knowledge, the best available solution for longitudinal control is the slip ratio control with a computation of the optimal slip; this computation requires an estimation of the road conditions. To estimate in real-time the road conditions different algorithms can be considered [3-7].

The references [21-22] presented an approach to the longitudinal control of a single driven wheel, adopting a configuration based on an adherence estimator and a controller of the adherence gradient as shown by Fig. 3. These

proposals aim to offer comparable or competitive performance with respect to the existing solutions, while allowing a lighter tuning procedure than the system proposed by [1]. This approach has longitudinal control performance as good as, e.g., [3-7]; on the other hand, the approach proposed by [3-7] requires a heavier tuning campaign of the system. The experimental strategy allowed tests in the presence of sudden changes in the road, hard to achieve in [12]. References [13,15,17,19,20] work at prefixed (or unknown) slip ratios, therefore do not exploit (or do not prove they do) the available adherence offered by the road as well as the proposed approach. On the other hand, the scope of the references [21-22] is limited to the case of a traction drive with DC motor or motors.

The present work is devoted to extend the techniques proposed in [21-22] to AC drives, focusing the case of a PM axial-flux in-wheel motor. The experimental tests are based on a test bench allowing the hardware-in-the-loop study of the power train using the real time computation and actuation of the vehicle dynamic, taking into account arbitrary and on-line modifiable road conditions.

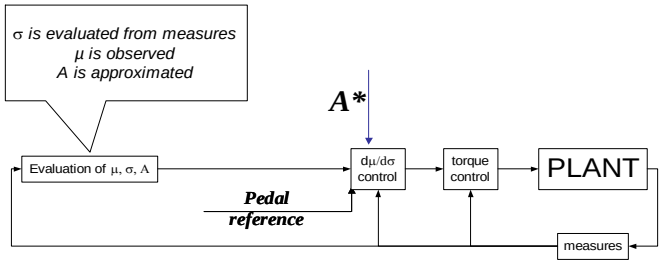

Fig. 3. Adherence gradient control

It is worth to mention that the longitudinal control of a vehicle with two driven wheel can be realized by duplicating the proposed system and sharing the same pedal reference and the same adherence gradient reference [3]; moreover, the duplicated proposed system can be used as a suitable actuator for a possible lateral control distinguishing the pedal references and the adherence gradient references.

II. Mathematical model of the driven wheel

This section presents briefly the mathematical model of the driven wheel of Fig. 4. The dynamic of a driven wheel is given by an equation of forces equilibrium:

$$T - R = M \frac{dV_{vehicle}}{dt}, \qquad (2)$$

and by an equation of torques equilibrium:

$$C_m - rT = J\frac{d\omega}{dt}, \tag{3}$$

the traction force is given by the normal force and the friction coefficient:

$$T = \mu \cdot N, \tag{4}$$

where R is the passive resistance to the vehicle motion, M is the vehicle mass, C_m is the motor torque applied on the tire, r is the tire radius, ω is the tire angular speed, J is the tire inertia, N is assumed as a quarter of the car weight, and in (1) $V_{tire} = \omega r$ holds.

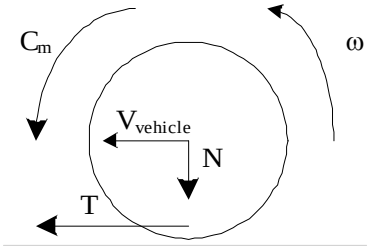

Fig. 4. Driven wheel.

The above model has to be completed by the road-tire friction characteristic $\mu(\sigma)$ of Fig. 2 that depends strongly on the operating conditions. Namely, the actual $\mu(\sigma)$ law depends on the tire slip angle, on the steering angle, on the road and tire conditions and, finally, on the speed. Figure 5 reports typical trends of the function $\mu(\sigma)$ for various road conditions, with a zero slip angle. These trends illustrate that some amount of slip is necessary to produce longitudinal tire-road force; on the other hand, the trends show an excessive slip leads to a loss of driving force, with high power losses and wear due to the friction.. Moreover, an example of the side friction coefficient μ_s is also reported in Fig. 5; its decreasing trend indicates the slip has to be limited to guarantee the lateral guidance of the vehicle.

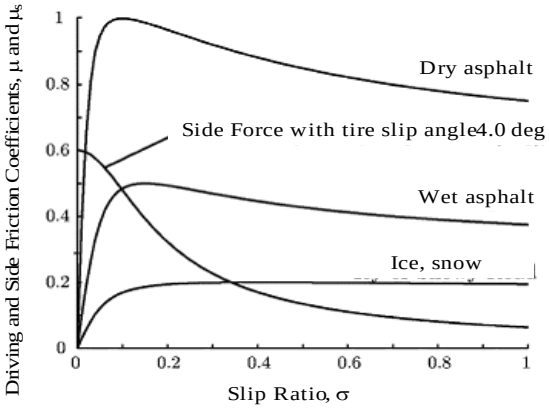

Fig. 5. Typical trends of longitudinal and side friction coefficients.

The work considers Permanent Magnet Synchronous motors, therefore, the torque production is ruled by the equations in the rotating frame:

$$\begin{cases} v_d = ri_d - p\omega_r\psi_q + \dfrac{d}{dt}\psi_d \\ v_q = ri_q + p\omega_r\psi_d + \dfrac{d}{dt}\psi_q \\ \psi_d = L_d i_d + \psi_{PM} \\ \psi_q = L_q i_q \\ T_e = \dfrac{3}{2} p\left(i_q\psi_{PM} + \left(L_d - L_q\right) i_q i_d\right) \end{cases}, \qquad (5)$$

where v_d and v_q represent the d and q-axis components of the motor voltage, i_d and i_q are the components of the motor current, ψ_d and ψ_q are the components of the flux linkage, ψ_{PM} represents the flux of the magnets, T_e is the electromagnetic torque, ω_r is the shaft speed r, p, L_d and L_q are motor parameters.

III. Adherence estimation

This Section presents the observer used to estimate the actual driving friction coefficient μ. The actual dynamic gives:

$$T = \frac{C_m - J\dot{\omega}}{r}. \qquad (6)$$

Let $\hat{T}$ an estimate of the adherence force, the estimation error is:

$$e = \hat{T} - T = \hat{T} - \frac{C_m - J\dot{\omega}}{r}. \qquad (7)$$

The desired error dynamic is:

$$\dot{e} + Ke = 0. \qquad (8)$$

The following equation can be obtained substituting (7) into (8) and supposing piecewise $\dot{T} = 0$:

$$\dot{\hat{T}} + K\left(\hat{T} - \frac{C_m - J\dot{\omega}}{r}\right) = 0. \qquad (9)$$

Previous relationship leads to the block scheme of Fig. 6. Figure 7 reports the simulated observer output responding to a step in the adherence and a step in the motor torque. The data show the observed driving force converges soon to the actual value and it is insensitive to a torque step.

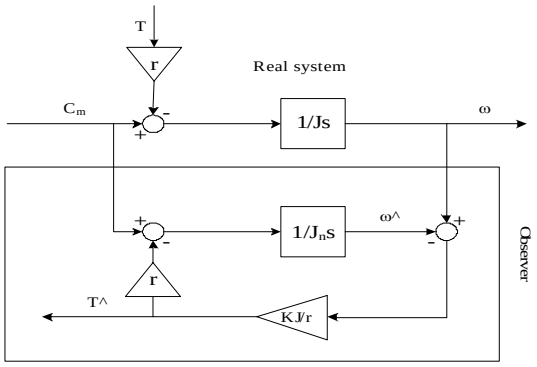

Fig. 6. Driving friction force observer.

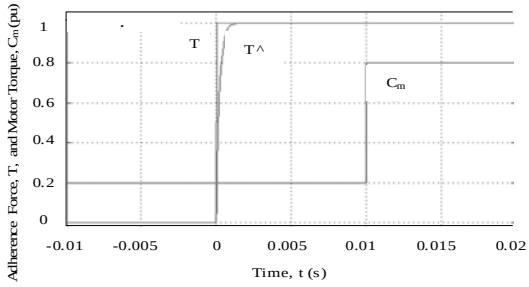

Fig. 7. Observer step response.

IV. Traction control

This Section shows how to estimate the adherence gradient *A*, then presents the sliding mode controller.

A. Evaluation of the adherence-slip gradient

The target of this TC is to operate at an assigned value of *A*, thus its correct estimation is critical. In dynamic conditions, *A* may be estimated by means of the ratio:

$$\frac{\Delta\mu}{\Delta\sigma} = \frac{\Delta\mu/\Delta t}{\Delta\sigma/\Delta t}. \qquad (10)$$

To compute the gradient, the proposed algorithm updates the ratio just when the amplitude of $\Delta\sigma$ is appreciable.

B. Sliding Mode Adherence Gradient Control

The region of the state space where *A*=0 is the desired sliding manifold. Based on the typical $\mu(\sigma)$ curves reported in Fig. 5 let us suppose that the actual $\mu(\sigma)$ curve presents a maximum; consequently, the $A(\sigma)$ is a decreasing function of σ,

$$dA/d\sigma < 0, \qquad (11)$$

at least close to the maximum. If the vehicle speed $V_{vehicle}$ can be considered constant, (1) gives:

$$sign(\dot{\sigma}) = sign(\dot{\omega}). \qquad (12)$$

The equations (11) and (12) give:

$$sign(\dot{A}) = -sign(\dot{\omega}). \qquad (13)$$

Moreover, according to the model of Section II, with $\sigma > 0, V_{vehicle} > 0$, for some values of the torque such as $C_m = \overline{C}_m > Tr$:

$$sign(\dot{\omega}) = \begin{cases} +1 \text{ if } C_m = \overline{C}_m \\ -1 \text{ if } C_m = 0 \end{cases}. \qquad (14)$$

Consequently, considering C_m the controlling quantity and adopting the discontinuous control:

$$C_m = \begin{cases} \overline{C}_m \text{ if } A > 0 \\ 0 \text{ if } A < 0 \end{cases}, \qquad (15)$$

from (13), (14) and (15) $A\dot{A} < 0$ will result, enforcing sliding mode on the manifold *A*=0 [14].

Because the above discontinuous control is affected by the current control loop dynamic, it would lead the wheel speed to chatter. Instead, the boundary layer technique is adopted to alleviate the chattering [14]. A sliding mode current control loop assists the adherence gradient control loop as showed by Fig. 8.

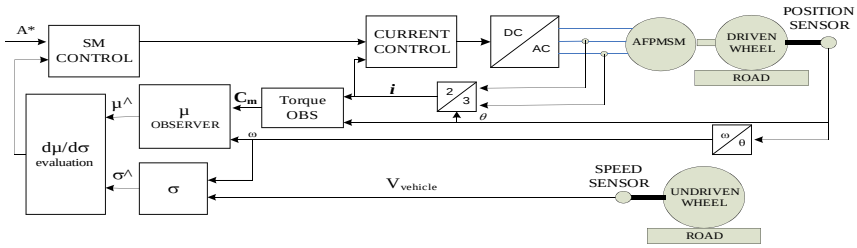

Fig. 8. Block scheme of the system with sliding mode adherence gradient control.

V. Test bench

To tune and verify the antiskid traction controller the authors arranged a test bench in the “Giovanni D'Angelo” Laboratory of Industrial Electronics, The University of Cassino. The test bench is based on the real time computation and actuation of the wheel dynamic, and consists of the following items as shown also by the block scheme of Fig. 9-a. The image of the electrical machines included in the test bench is reported in Fig. 9-b.

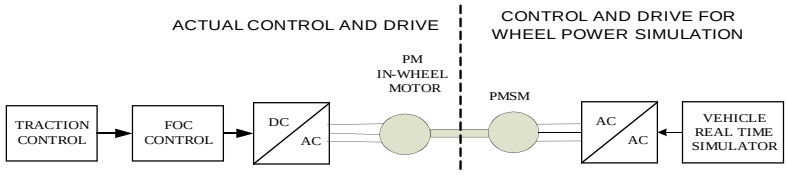

Fig. 9-a. Block scheme of the test bench.

Fig. 9-b. Electrical machines in the test bench.

- Items under test.

1. Actual control hardware.
2. Actual DC/DC power converter.
3. Actual DC motor.

- Wheel hardware-in-the-loop simulator.

1. Control hardware for the real-time computation of the wheel dynamic, including the adherence.
2. Power inverter.
3. machine loading the actual motor.

This bench can reproduce arbitrary adherence-slip curves and can modify them in running. The simulator imposes in real-time the motor speed foreseen by the vehicle equations. The simulator can set the axle speed in any likely operating condition, thanks to its torque and bandwidth performances.

VI. Experimental results

This Section intends to prove the functionality of the proposed approach. The case of a light vehicle on a slippery surface was taken into consideration and tested by means of the above described test bench. The first piece of information, reported in Fig. 10, records that without traction control, in presence of a step pedal command, the wheel slips and its speed is limited only by the protection of the bench. In the same conditions, the vehicle with traction control starts correctly as evidenced by the speed curves in Fig. 11. Figure 12 illustrates the operation of the controller showing the reference (black) and actual (gray) torque component of the current. Figure 13 records the torques applied to the wheel by the road (adherence) and by the motor. Figures 14 and 16 are two zooms of Fig. 17, and Figures 15 and 17 depict the corresponding motor phase currents. These last four figures show how the intervention of the traction controller modify the motor currents.

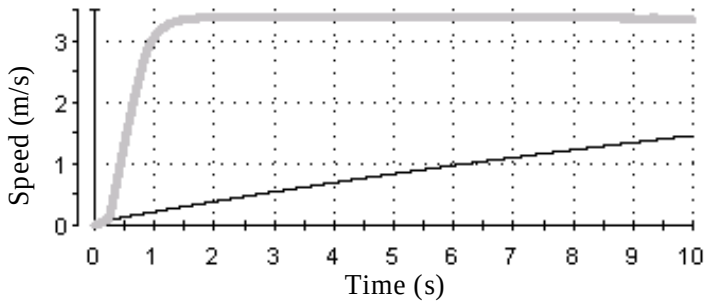

Fig. 10. Linear speeds of tire (gray) and vehicle (black) without traction control.

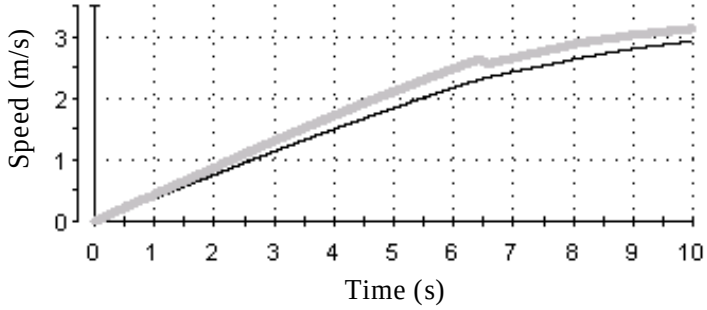

Fig. 11. Linear speeds of tire (gray) and vehicle (black) with traction control.

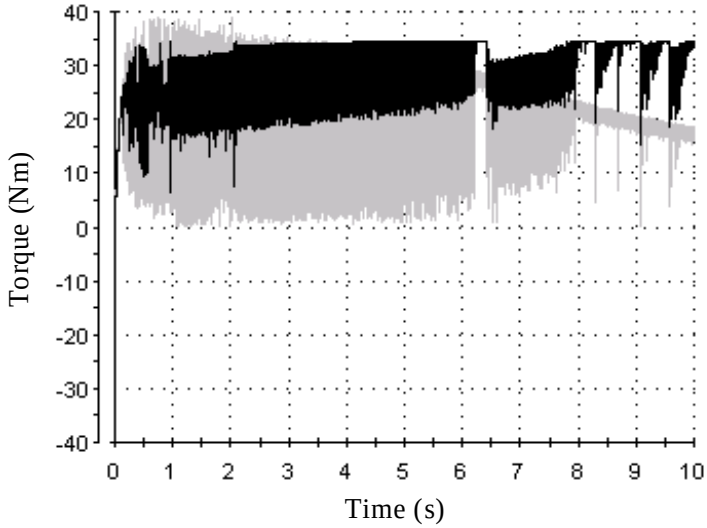

Fig. 12. Reference (black) and actual (gray) torque component of the current.

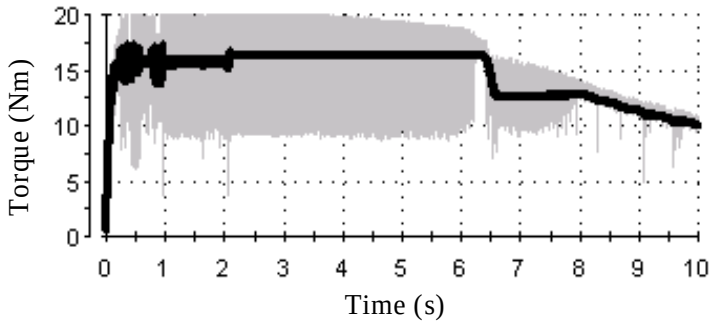

Fig. 13. Motor (gray) and adherence (black) torques applied on the wheel.

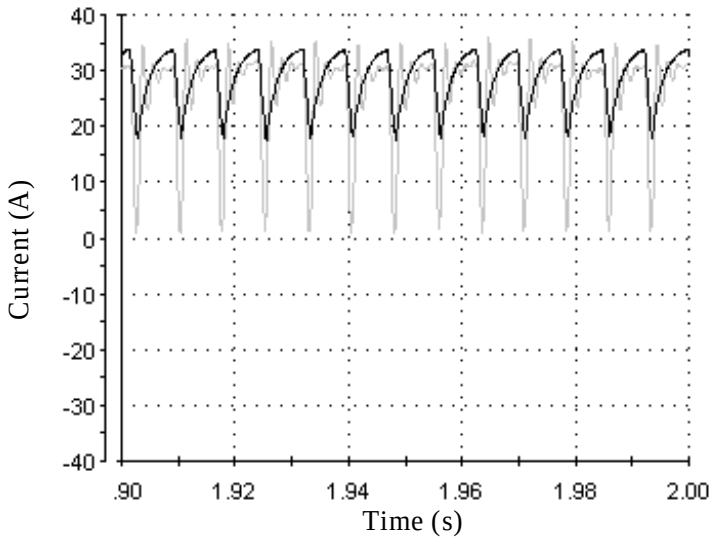

Fig. 14. Reference (black) and actual (gray) torque component of the current.

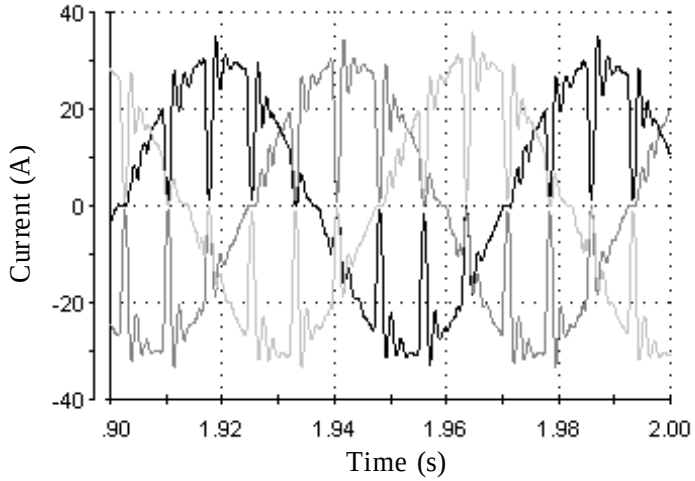

Fig. 15. Motor phase currents.

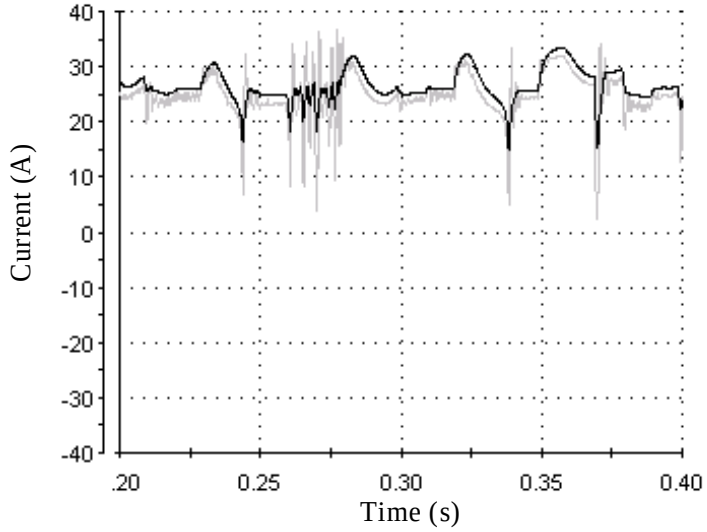

Fig. 16. Reference (black) and actual (gray) torque component of the current.

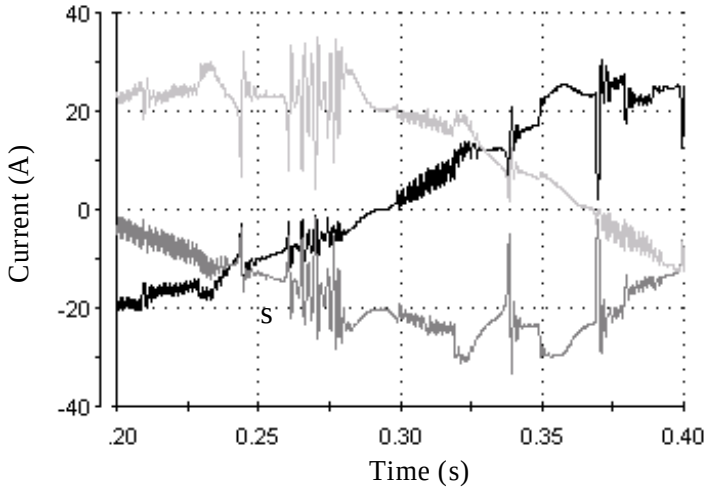

Fig. 17. Motor phase currents.

VII. Conclusions

This work extended to the PM AC case a method already proposed for DC motors. The paper considered an approach to the longitudinal control of a single wheel adopting a configuration based on an adherence estimator and a sliding mode controller of the adherence gradient. The test rig computes the vehicle dynamics in real-time and loads accordingly the drive under test. The proposed controller does not require any knowledge of the road conditions and is capable of properly reacting to sudden changes of the adherence. The controller was verified by means of experimental tests showing its functionality.

References

[1] Chan, C.C.; Wong, Y.S.; "Electric vehicles charge forward," *IEEE Power and Energy Magazine*, Volume 2, Issue 6, Nov.-Dec. 2004 Page(s):24 - 33

[2] Wehrey, M.C.; "What's new with hybrid electric vehicles," *IEEE Power and Energy Magazine*, Volume 2, Issue 6, Nov.-Dec. 2004 Page(s):34 - 39

[3] Y. Hori, "Future Vehicle Driven by Electricity and Control — "Research on Four-Wheel-Motored, "UOT Electric March II"," *IEEE Trans. Ind. Electr.*, vol. 51, N. 5, Oct. 2004. Pages: 954 - 962.

[4] S. Sakai, H. Sado, and Y. Hori, "Motion Control in an Electric Vehicle with Four Independently Driven In-Wheel Motors,", I*EEE/ASME Trans. Mech.*, vol. 4, N. 1, March 1999. Pages: 9 - 16.

[5] H. Sado, S. Sakai, Y. Hori, “Road Condition Estimation for Traction Control in Electric Vehicle,” Proceedings of the IEEE International Symposium on Industrial Electronics, 1999. ISIE ‘99, Volume: 2, 12-16 July 1999. Pages: 973 – 978.

[6] Y. Hori, Y. Toyoda, and Y. Tsuruoka, “Traction Control of Electric Vehicle: Basic Experimental Results Using the Test EV “UOT Electric March”,” *IEEE Trans. Ind. App*., vol. 34, N. 5, Sept./Oct. 1998. Pages: 1131-1138.

[7] K. Furukawa, Y. Hori, “Recent Development of road condition estimation techniques for electric vehicle and their experimental evaluation using the test EV “UOT March I and II”,”. The 29th Annual Conference of the IEEE Industrial Electronics Society, 2003. IECON '03. , Volume: 1, 2-6 Nov. 2003. Pages: 925 – 930.

[8] Laura R. Ray, “Nonlinear State and Tire Force Estimation for Advanced Vehicle Control,” *IEEE Trans. Control Systems Tech.*, vol. 3, N. 1, March 1995. Pages: 117 – 124.

[9] Laura R. Ray, “Real-Time determination of road coefficient of friction for IVHS and advanced vehicle control,” *Proc. American Control Conference*, Seattle, Washington, Volume: 3, 21-23 June 1995. Pages: 2133 - 2137.

[10] Laura R. Ray, “EXPERIMENTAL DETERMINATION OF TIRE FORCES AND ROAD FRICTION,” *Proc. American Control Conference*, Philadelphia, Pennsylvania, Volume: 3, 24-26 June 1998. Pages: 1843 – 1847.

[11] P. Marino, S. Meo, M. Scarano, “A stochastic controller for anti-skidding microprocessor system,” Fifth European Conference on Power Electronics and Applications, 1993, EPE93, 13-16 Sep 1993. Pages: 162 - 166 vol.6.

[12] P. Khatun, C. M. Bingham, N. Schofield, and P. H. Mellor, “Application of Fuzzy Control Algorithms for Electric Vehicle Antilock Braking/Traction Control Systems,” *IEEE Trans. Veich. Tech.*, vol. 52, N. 5, Sept. 2003, pp. 1356-1364.

[13] R. Pusca, Y. Ait-Amirat, A. Berthon, J.-M. Kauffmann, “Fuzzy-logic-based control applied to a hybrid electric vehicle with four separate wheel drives,” *IEE Proc.-Control Theory Appl.*, vol. 151, N. 1, January 2004. Pages: 73 – 81.

[14] V. Utkin, J. Guldner, J. Shi, *Sliding Mode Control in Electromechanical Systems.* London, UK: Taylor&Francis, 1999, Chaperts 3 and 8.

[15] S. Kawasaki, S. Ouchi, “Traction control for automobiles by model-following sliding mode control,” Proceedings of the 41st SICE Annual Conference , SICE 2002, Volume: 2 , 5-7 Aug. 2002. Pages: 1175 – 1180.

[16] M. Jalili-Kharaajoo, F. Besharati, “Sliding mode traction control of an electric vehicle with four separate wheel drives,” IEEE Conference Emerging Technologies and Factory Automation Proceedings, 2003. ETFA '03. , Volume: 2 , 16-19 Sept. 2003. Pages: 291 – 296.

[17] Hung Pham, K. Hedrick, M. Tomizuka, “Combined lateral and longitudinal control of vehicles for IVHS,” American Control Conference, 1994 , Volume: 2 , 29 June-1 July 1994. Pages: 1205 – 1206.

[18] E. de Santis “”VED” EV Torque Control: Design and Test of a fuzzy antiskid control,” (in Italian,) Laurea dissertation, Fac. Elect. Eng., University of Cassino, Cassino, Italy, 2005.

[19] Chunting Mi; Hui Lin; Yi Zhang; “Iterative learning control of antilock braking of electric and hybrid vehicles,” *IEEE Transactions on Vehicular Technology*, Volume 54, Issue 2, March 2005 Page(s):486 - 494

[20] Fujimoto, H.; Saito, T.; Tsumasaka, A.; Noguchi, T.; “Motion control and road condition estimation of electric vehicles with two in-wheel motors,” *Proceedings of the 2004 IEEE International Conference on Control Applications*, 2004. Volume 2, 2-4 Sept. 2004 Page(s):1266 - 1271 Vol.2

[21] V. Delli Colli, G. Tomassi, M. Scarano; “Fuzzy longitudinal traction control,” *Advanced Intelligent Mechatronics. Proceedings*, 2005 IEEE/ASME International Conference on July 24-28, 2005 Page(s):289 - 294

[22] V. Delli Colli, G. Tomassi, M. Scarano; ““Single Wheel” Longitudinal Traction Control for Electric Vehicles”, *IEEE Transactions on Power Electronics*, May 2006.